Transactions of the **14th International Conference on Structural Mechanics in Reactor Technology** (SMiRT 14), Lyon, France, August 17-22, 1997

**HKW/13**

# Seismic analysis of a RC shear wall

**Hasegawa T.[1], Kumagai H.[1], Irino K.[1], Rots J.G.[2], Feenstra P.H.[2]**
*(1) Shimizu Corporation, Japan*
*(2) TNO Building and Construction Research, The Netherlands*

## Abstract

The paper discusses the finite element simulation with the finite element system DIANA of a large-scale experiment on a reinforced concrete shear wall. The simulation shows that useful information on the failure mode can be obtained from the nonlinear static, and nonlinear transient dynamic analysis.

## 1 Introduction

Since 1986, the Nuclear Power Engineering Corporation (NUPEC) has been conducting a project entrusted by the Ministry of International Trade and Industry (MITI) entitled "Elastoplastic Test of Reactor Buildings". As part of the project, the "Seismic Ultimate Dynamic Response Test" was carried out using a large scale, high performance shaking table at NUPEC's Tadotsu Engineering Laboratory in 1991. This experiment has been the subject of an International Standard Problem (ISP) where the numerical simulation of this experiment was the primary goal, [1].

The problem has been analyzed in a joint research program by Shimizu Corporation and TNO Building and Construction Research, and this paper discusses the contribution to the ISP briefly. See for more information about the analysis [2].

## 2 Finite element model

**Governing equations** The system of governing equations for a nonlinear transient dynamic problem at time $t$ can be given as

$$\mathbf{M}\ddot{\mathbf{u}}_{t+\Delta t} + \mathbf{C}\dot{\mathbf{u}}_{t+\Delta t} + \mathbf{K}\mathbf{u}_{t+\Delta t} = -\mathbf{M}\ddot{\mathbf{u}}_{\mathrm{su}}(t+\Delta t) \tag{1}$$

where $\mathbf{u}$ is the relative response to fixed "ground" point and the external loading due to the base excitation is given by $\mathbf{M}\ddot{\mathbf{u}}_{\mathrm{su}}(t+\Delta t)$ in which $\ddot{\mathbf{u}}_{\mathrm{su}}$ the applied base acceleration vector. The symbols $\mathbf{M}$, $\mathbf{C}$, and $\mathbf{K}$ are the mass matrix, the damping matrix, and the stiffness matrix respectively.

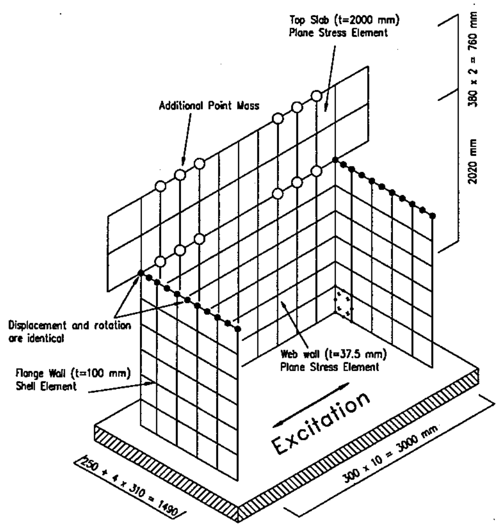


Figure 1: Finite element discretization of shear wall

In practice the presence of damping reduces the steady state response and damps out the transient response. This physical aspect has to be taken in account in most analysis to get reliable results. A viscous type of damping is used, which means a damping proportional to the velocity, with a Rayleigh-type of damping given by.

$$\mathbf{C} = a\mathbf{M} + b\mathbf{K} \tag{2}$$

where $a$ and $b$ are constants to be determined from given or desired damping ratios of two natural frequencies.

**Discretization** The finite element discretization is depicted in Figure 1. The structure is discretized with 84 quadratic plane–stress elements with a four-point quadrature to model the web, and 60 quadratic shell elements with a four-point quadrature in-plane and a three-point integration out-of-plane to model the flanges. Because of symmetry only half of the structure is modeled. Twelve point–mass elements are used to model the additional weight of the top slab. The reinforcement in the web and in the flanges is modeled with embedded reinforcement grids with the appropriate cross-sectional properties, [1, 2].

The base slab has not been modeled because it is assumed that the very stiff base slab can be replaced by fixed supports. The horizontal base acceleration is applied by prescribing the simultaneous horizontal acceleration of all the fixed supports.

**Constitutive modeling** The top slab is modeled with a linear-elastic material model with a Young's modulus, $E_c$ = 23000 [MPa] and a Poisson's ratio $\nu$ = 0.16 [−]. The web and the flanges are modeled with a combined cracking-crushing model in order to simulate the expected failure mode of the structure: extensive cracking and ultimately compressive-shear failure of the web. The combined failure surface is shown in Figure 2. The Young's modulus and Poisson's ratio are chosen equal to the elastic properties of the top slab. The tensile strength is $f_{ct}$ = 2.24 [MPa] and the compressive strength is $f_{cc}$ =

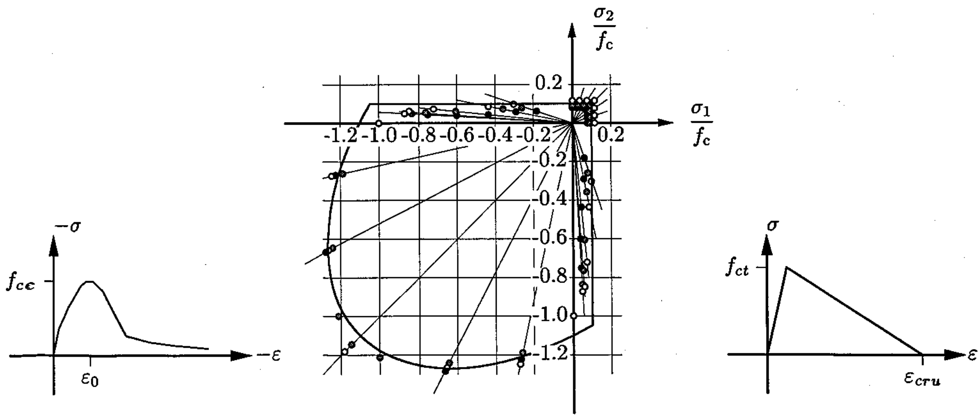

Figure 2: Biaxial failure surface with plane stress data of Kupfer and Gerstle

23.0 [MPa]. The tensile failure behavior is modeled with a fixed smeared crack model with linear tension-softening with an ultimate crack strain, $\varepsilon_{cru} = 0.5\ \varepsilon_{sy}$, where $\varepsilon_{sy}$ is the yield strain of the embedded reinforcement. The shear-retention factor $\beta$ is equal to one percent. The compressive failure behavior is modeled with a Von Mises plasticity model with a compression-softening model according to Figure 2. The compressive stress-strain relation is given by a hardening/softening relation with a peak strain $\varepsilon_0 = 0.0025$ [−].

The reinforcement is modeled with an elastoplastic model with isotropic hardening. The Young's modulus $E_s = 185000$ [MPa] and the yield strength $f_{sy} = 383$ [MPa] with maximum strength of 482 [MPa] at an elongation of 29.2 %.

# 3 Analysis

The purpose of the simulation of the experiment is the prediction of the proper failure mode in a seismic analysis. Before the transient analysis is performed, the eigenvalues of the linear, undamped, system are calculated and a static nonlinear analysis is carried out.

**Eigenvalue analysis** The eigenvalue analysis is performed for a twofold purpose, firstly to check the finite element model, and secondly to determine the parameters $a$ and $b$ of the Rayleigh damping matrix. The first five eigenmodes are determined which are expected to be representative for the structure. The last two eigenmodes with eigenfrequencies $f_4 = 82.8$ [Hz] and $f_5 = 82.9$ [Hz] are very close and are the bending modes of the flanges. The first three eigenmodes with $f_1 = 13.9$ [Hz], $f_2 = 40.9$ [Hz], and $f_3 = 57.6$ [Hz] are shown in Figure 3. The eigenmodes are respectively shear deformation, vertical swaying, and rocking. The damping parameters which are determined by fitting on the experimental values are shown in Figure 4. It is clear that the first three eigenfrequencies are all damped with approximately 2 % of the critical damping.

**Static nonlinear analysis** The static analysis is performed to study the ultimate load carrying capacity and the post-failure behavior in a static analysis. The numerical results

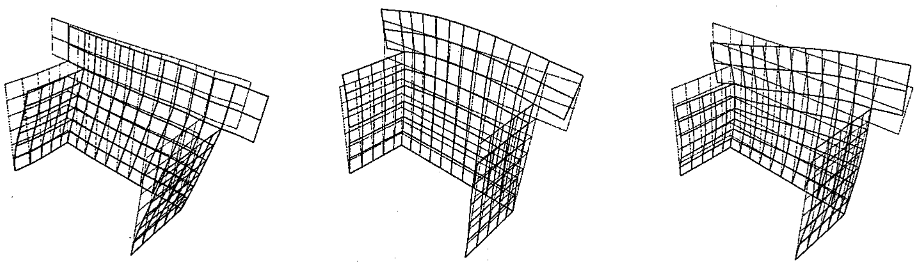

$f_1 = 13.9$ [Hz] $f_2 = 40.9$ [Hz] $f_3 = 57.6$ [Hz]

Figure 3: Eigenmodes of linear structure

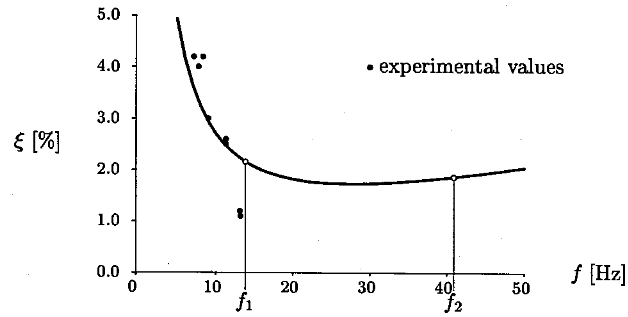


Figure 4: Damping behavior with $a = 3.0$ and $b = 0.0001$

are compared with the data given in the experimental results [1] in which a pseudo-static force is determined from the experimental accelerations, see Figure 5. The initial stiffness

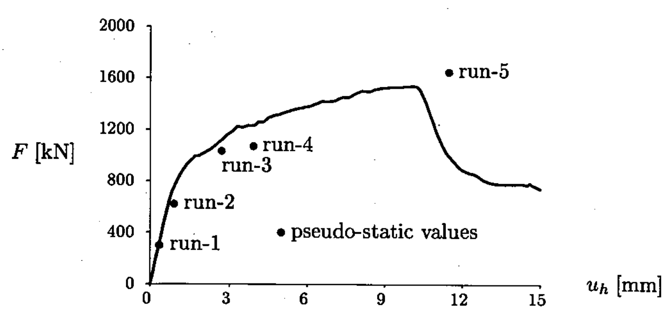


Figure 5: Load–displacement curve static analysis

of the analysis is in accordance with the initial stiffness of the experiment. At a shear force of approximately 800 [kN] the stiffness reduces due to extensive cracking, both in the web as well as in the flanges. At the maximum load of approximately 1500 [kN] the load carrying capacity of the structure reduces, which is caused by compression softening of the right toe of the web.

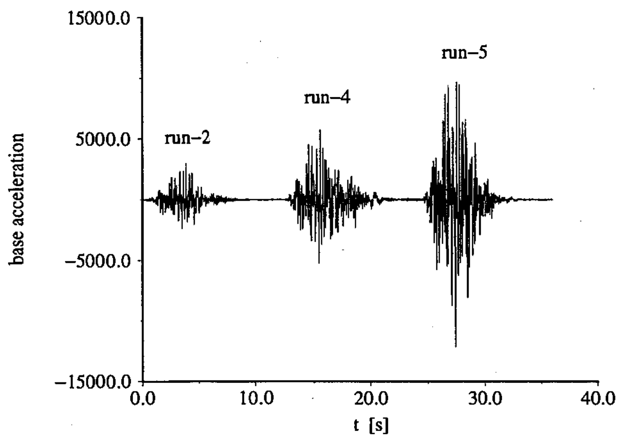


Figure 6: Base acceleration diagram

**Transient nonlinear analysis** The input waves for the transient analysis are determined by a generated, artificial signal according to a target response spectrum and a Jenning's envelope of the amplitude [1]. The experimental program consists of five levels, run-1, run-2, run-3, run-4, and run-5, in which the amplitude is increased in each sequential run. The target levels at each run correspond to a specific type of damage of the structure, see also Figure 5. The numerical analysis is performed with three levels, run-2, run-4, and run-5 because it is assumed that the intermediate levels do not contribute significantly to the failure of the shear wall. The generated base acceleration diagram is given in Figure 6.

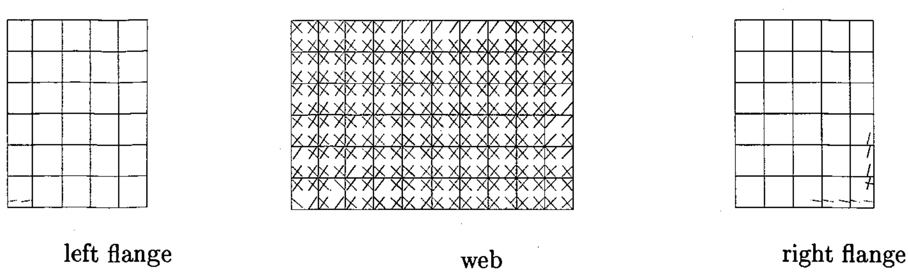


Figure 7: Crack pattern after run-2

The loading of run-2 results in extensive cracking of the web, but the compressive stresses are all lower than the maximum compressive strength, see Figure 7. During run-4 the flanges are also cracked, see Figure 8, and the compressive stresses almost violate the ultimate compressive strength. Run-5 causes imminent failure of the specimen with a compressive-shear failure mechanism as can be observed from Figure 10. The flanges are progressively cracks, see Figure 9 and the reinforcement is yielding in a large area, see Figure 11.

The comparisons of the acceleration and the displacement of the top slab with the

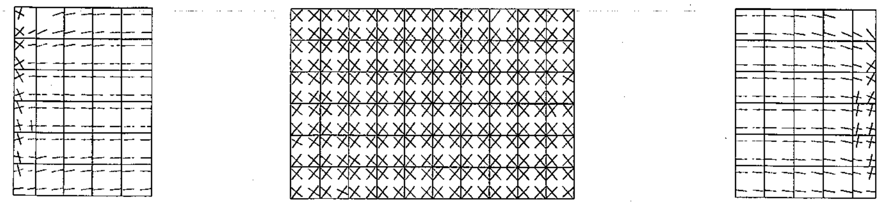

left flange web right flange

Figure 8: Crack pattern after run-4

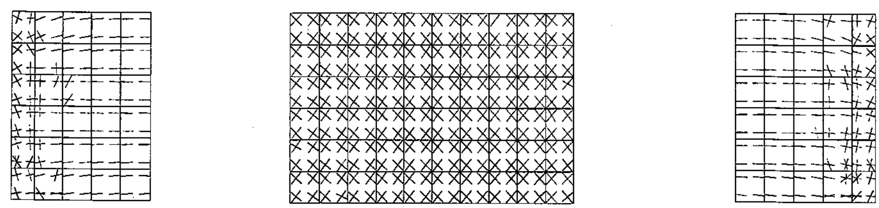

left flange web right flange

Figure 9: Crack pattern at failure

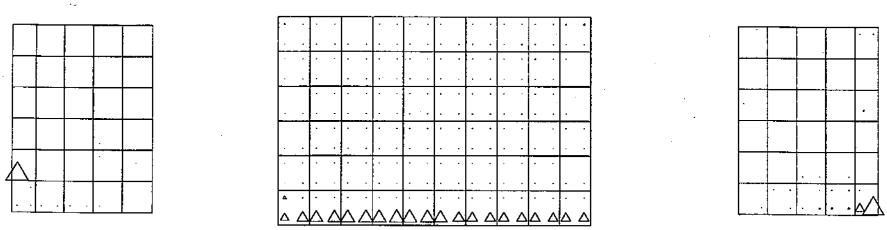

left flange web right flange

Figure 10: Crushed area at failure

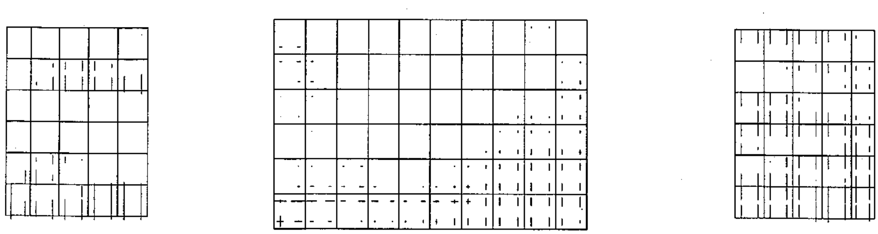

left flange web right flange

Figure 11: Yielding of reinforcement at failure

experiment are shown in Figures 12 and 13. Up to failure, the calculated accelerations and the calculated displacements are in agreement with the experimental behavior. The

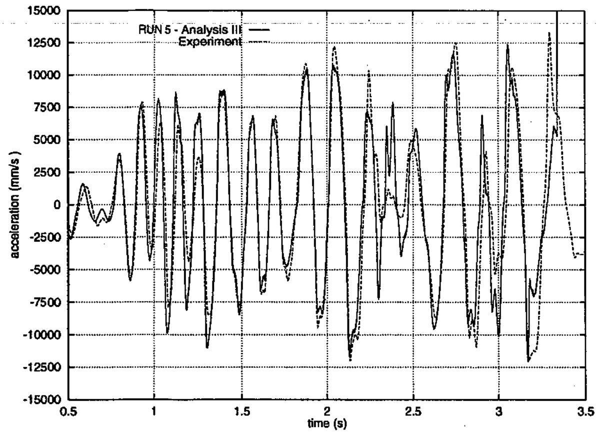


Figure 12: Acceleration top slab RUN 5

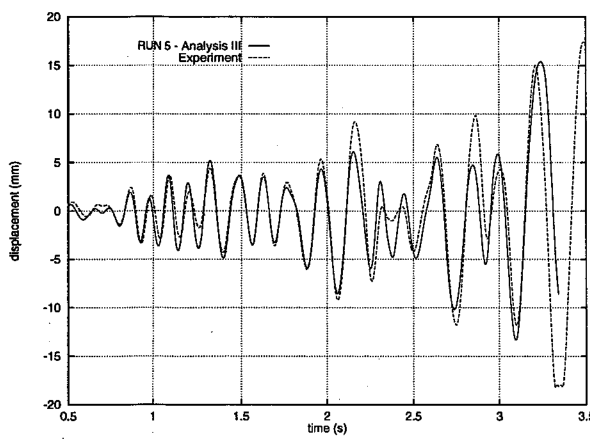


Figure 13: Displacement top slab RUN 5

calculations have been terminated at the stage where no converged solution could be found. At this stage the stress in crushed area, see Figure 10, are all in the tail of the softening diagram, see Figure 2, left $\sigma$-$\varepsilon$ diagram.

The lowest eigenfrequency will reduce due to the increasing damage after each run as has been observed in the experiment. This phenomenon is also observed during the analysis. The lowest eigenfrequency of the linear-elastic structure is calculated as $f_1 =$ 13.9 [Hz] whereas in the experiment a lowest eigenfrequency of 13.1 [Hz] is found. After run-2, which causes extensive cracking of the web, the analysis shows a reduction of the lowest eigenfrequency to 12.7 [Hz] whereas in the experiment 11.3 [Hz] is found. After run-4 the lowest eigenfrequency is further reduced to 8.5 [Hz] with an experimental value of 7.1 [Hz]. The numerical lowest eigenfrequencies are overestimated compared with the experimental lowest values slightly, which can be explained by the increasing damping due to reduction of the stiffness of the structure. In the analysis the damping is determined on the basis of the linear-elastic eigenvalue analysis and will probably underestimate the damping in the damaged structure. This is also clear from the FFT transform of the experimental and numerical response, see Figure 14.

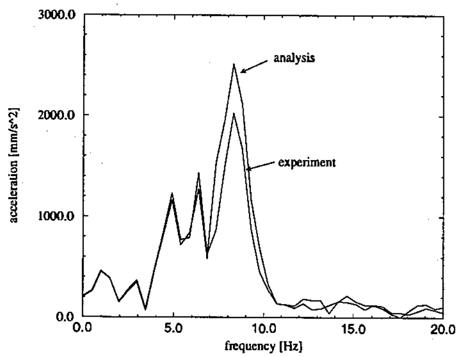


Figure 14: Fourier transform response run-5

# 4 Concluding remarks

In conclusion, the analysis of these types of structures is possible with a general purpose finite element system as DIANA. The tools which are available, such as eigenvalue analysis, static nonlinear analysis, and transient nonlinear analysis, provide as versatile tool box for seismic analysis of concrete structures. The agreement between experimental results and numerical results is satisfactory and useful for practical applications.

# 5 Acknowledgments


The calculations have been carried out by mr. H.H.J. Bremer as a part of his graduation work at Delft University of Technology under supervision of Prof. J. Blaauwendraad with the finite element system DIANA Release 6.2. Mr. P. Nauta of TNO Building and Construction Research is greatly acknowledged for his contribution in the modeling and dynamic analysis.


# References


[1] Specification Report of Seismic Shear Wall ISP on NUPEC's Seismic Ultimate Dynamic Response Test. Committee on the Safety of Nuclear Installations, Nuclear Power Engineering Corporation. nr. NU–SSWISP–D009, Japan , 1994.

[2] H. H. J. Bremer. Seismic analysis of a shear wall. Technical Report 96-NM-R0984, TNO Building and Construction Research, Rijswijk, 1996.